Table 3 Comparison of present with previous perfect gas results[a]

Altitude, kft →	70	100	120	170	200	220	250	280
Velocity × 10^{-3} →	36	26	40	35	26	28	45	32
M_1	0.33	−1.19	−1.95	−2.13	0.92	1.97	3.57	4.46
ρ_s/ρ_1	−0.79	0.24	−0.86	−0.49	−0.56	−0.49	−0.73	0.14
p_s/p_1	0.44	−2.47	−4.03	−4.35	1.70	3.79	7.10	8.98
T_s/T_1	1.38	−2.64	−3.41	−3.75	2.62	4.56	7.93	8.96
H_s/H_1	1.03	−1.99	−3.53	−3.85	2.17	4.33	7.64	9.46
H_0/H_1	1.09	−1.96	−3.47	−3.83	2.23	4.38	7.66	9.50
p_0'/p_1	0.44	−2.52	−4.07	−4.35	1.67	11.6	7.12	8.92
T_0'/T_1	1.34	−2.54	−3.35	−3.71	2.59	8.83	7.97	8.97

[a] Data shown were computed from percent difference = 100 [x(Marrone) − x(present results)]/x(present results).

mal shock stagnation conditions. The data were presented in graphical and tabular form over the ranges of alt = 10^4-$(10^3)4 \times 10^5$ ft and velocity = 6000(1000)50,000 fps. The calculations were based on the imperfect air thermodynamic properties of Hilsenrath and Klein[5] and Lewis and Neel[6] and the 1962 U. S. Standard Atmosphere.[7]

Some of the results of the calculations are shown on Figs. 1–3. The sphere stagnation heat-transfer rates were computed from the Fay and Riddell formula[8] in the form used previously by Lewis and Burgess[9]:

$$\dot{q}(r_n)^{1/2} = 7.55274 \times 10^{-3}(\rho_w\mu_w)^{0.1}(\rho_0'\mu_0')^{0.4}(H_0 - H_w)(p_0'/\rho_0')^{0.25}$$

in Btu(in.)$^{1/2}$/ft^2-sec. The viscosity data were obtained from Hansen;[10] Lewis number was assumed unity, the sphere radius is in inches, and w and 0′ denote wall (T_w = 300°K) and normal shock stagnation conditions.

Table 1 shows the ranges of conditions considered in the imperfect gas calculations of Lewis and Burgess and two previous perfect gas calculations of Wittliff and Curtis[2] and Marrone.[3] As noted in the table, the freestream stagnation conditions were not presented in the earlier perfect gas results, and it is these data that are most affected by imperfect gas effects.

A comparison was made between the 1959 Air Research and Development Command (ARDC) model[11] and the 1962 standard atmosphere used in the present work, and the results are shown in Table 2. The differences near 220,000 ft are as large as 15% and affect the normal shock solutions.

A comparison was made between the present results and those of Marrone[3] based on the 1959 model atmosphere. The results of that comparison are shown in Table 3. The differences shown in Table 3 are mainly due to differences in the standard atmospheres and are not due to imperfect gas effects since the densities are too low for these effects to be important. The freestream stagnation conditions shown on Fig. 1 above about 100 atm are, however, affected by imperfect gas effects.

The present results are based on the most recent thermodynamic data and model atmosphere known to the authors. Differences of about 10% were indicated in normal shock wave properties when compared with previous perfect gas results. These results are considered significant and the tabulated data in Ref. 4 are designed to permit easy interpolation.

References

[1] Feldman, S., "Hypersonic gas dynamic charts for equilibrium air," Avco-Everett Research Rept. 40 (1957).

[2] Wittliff, C. E. and Curtis, J. T., "Normal shock wave parameters in equilibrium air," Cornell Aeronautical Lab. Rept. CAL-111 (1961).

[3] Marrone, P. V., "Normal shock waves in air: Equilibrium composition and flow parameters for velocities from 26,000 to 50,000 ft/sec," Cornell Aeronautical Lab. Rept. AG-1729-A-2 (1962).

[4] Lewis, C. H. and Burgess, E. G., III., "Altitude-velocity table and charts for imperfect air," Arnold Engineering Development Center TDR-64-214 (1964).

[5] Hilsenrath, J. and Klein, M., "Tables of thermodynamic properties of air in chemical equilibrium including second virial corrections from 1500°K to 15,000°K.," Arnold Engineering Development Center TDR-63-161 (1963).

[6] Lewis, C. H. and Neel, C. A., "Thermodynamic properties for imperfect air and nitrogen to 15,000°K," AIAA J. 2, 1847–1849 (1964).

[7] *U. S. Standard Atmosphere, 1962* (U. S. Government Printing Office, Washington, D. C., 1962).

[8] Fay, J. and Riddell, F. R., "Theory of stagnation point heat transfer in dissociated air," J. Aerospace Sci. 25, 73–85, 121 (1958).

[9] Lewis, C. H. and Burgess, E. G., III, "Charts of sphere stagnation heat-transfer rate in air and nitrogen at high temperatures," Arnold Engineering Development Center TDR-63-139 (1963); also AIAA J. 1, 1927–1929 (1963).

[10] Hansen, C. F., "Approximation for the thermodynamic and transport properties of high-temperature air," NACA TN 4150 (1958).

[11] Minzner, R. A., Champion, K. S. W., and Pond, H. L., "The ARDC model atmosphere, 1959," Air Force Cambridge Research Labs. TR-59-267 (1959).

Vibration of Hub-Pin Plates

R. R. Craig* and H. J. Plass†
University of Texas, Austin, Texas

Previous investigations have presented experimental data for the mode shapes and frequencies of rectangular, triangular, and skewed cantilever plates.[1,2] Recent experimental studies have confirmed the results of previous tests on cantilevered plates and also provided vibration data for hub-pin plates. The frequencies and nodal patterns of a square cantilever plate, a square hub-pin plate, a 45° cantilever plate, and a 45° hub-pin plate are shown in Fig. 1. A dimensionless frequency parameter Ω is given, where

$\Omega = 2\pi f/(D/\rho h a^4)^{1/2}$
f = frequency in cps
D = plate stiffness = $Eh^3/12(1 - \nu^2)$
ρ = density
h = thickness
a = length of root chord

Detailed deflection data for the hub-pin plates vibrating in the indicated modes are available in Ref. 4.

The frequencies and mode shapes were obtained by use of an electromagnetic shaker and a capacitance deflection probe shown in Fig. 2. The rotational restraint pin and a

Received December 8, 1964. Supported by the Navy Bureau of Weapons as a part of Contract No. NOrd-16498.

* Assistant Professor of Engineering Mechanics and Research Engineer, Defense Research Laboratory. Member AIAA.

† Professor of Engineering Mechanics and Research Engineer (Consultant), Defense Research Laboratory.

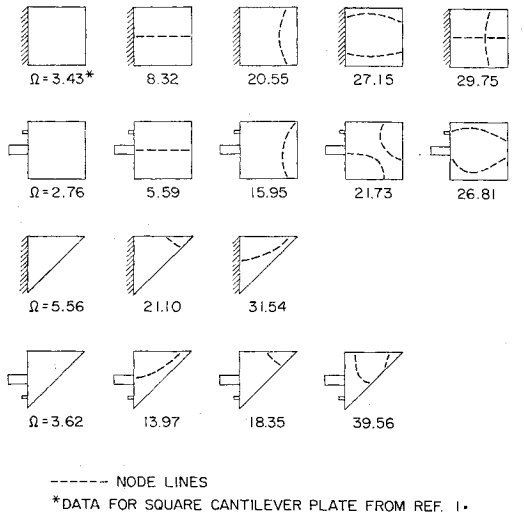

Fig. 1 Frequencies and nodal patterns for vibrating plates.

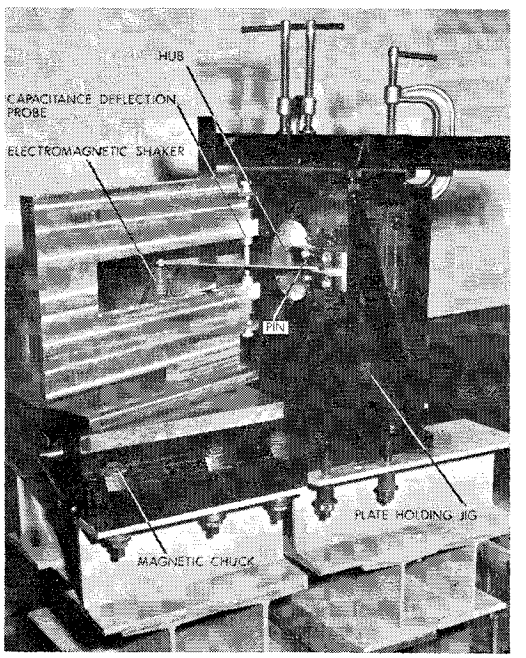

Fig. 2 Hub-pin plate mounting jig and capacitance deflection probe.

portion of the bearing-mounted hub may also be seen in Fig. 2. The deflection probe was supported by a magnetic chuck, which served to provide a rigid base and a convenient means of positioning the probe at various locations on the test plate. The entire deflection probe support was isolated from the base that supported the test plate and the electromagnetic shaker. The electromagnetic shaker and deflection probe are described more fully in Refs. 3 and 4.

References

[1] Barton, M. V., "Vibration of rectangular and skew cantilever plates," J. Appl. Mech. **18**, 129–134 (1951).

[2] Gustafson, P. N., Stokey, W. F., and Zorowski, C. F., "An experimental study of natural vibration of cantilevered triangular plates," J. Aerospace Sci. **20**, 331–337 (1953).

[3] Beck, C. W., "An excitation and instrumentation system for vibrating plate studies," Defense Research Lab. Rept. DRL-467, CF-2930, University of Texas, Austin, Texas (June 1961).

[4] Craig, R. R., Plass, H. J., and Caughfield, D. A., "Experimental determination of frequencies and mode shapes of cantilever and hub-pin plates," Defense Research Lab. Rept. DRL-518, CR-13, Univ. of Texas, Austin, Texas (June 1964).

Weak Radiation from a Hypersonic Shock

Inge L. Ryhming*
Aerospace Corporation, El Segundo, Calif.

A REGULAR shock in a one-dimensional supersonic flow may be regarded as a discontinuity in the temperature T, the velocity u, etc., such that the shock can be described in terms of step functions. However, a step-function behavior of the temperature of the medium produces a radiative heat flux. Assuming, for simplicity, that the medium is grey, the radiative flux can be calculated from the formula[1]

$$\bar{q}(\xi) = 2\sigma \int_{-\infty}^{+\infty} T^4 \operatorname{sgn}(\xi' - \xi) E_2(|\xi - \xi'|) d\xi' \quad (1)$$

which defines $\bar{q}(\xi)$ as a radiative flux in the negative x direction; σ is the Stefan-Boltzmann constant, ξ is the optical depth, and $E_2(x)$ is a particular form of the integro-exponential function $E_n(x)$ of general order n (see Ref. 1, p. 253). If the jump of a temperature step function is located at $\xi = 0$, one readily obtains from Eq. (1) the corresponding flux as given by the formula

$$\bar{q}(\xi) = 2\sigma [T^4]_0 E_3(|\xi|) \quad (2)$$

showing that $\bar{q}(\xi)$ is continuous and symmetric with respect to $\xi = 0$. In Eq. (2) the symbol $[\ ]_0$ stands for the jump in the quantity within the brackets across the discontinuity, i.e.,

$$[T^4]_0 = T_{0+}{}^4 - T_{0-}{}^4 \quad (3)$$

For a shock wave in cool air, the ratio of the maximum value of $\bar{q}$, which according to Eq. (2) occurs for $\xi = 0$, and the kinetic energy of the freestream, i.e., $\sigma[T^4]_0/\frac{1}{2}\rho_\infty U_\infty{}^3$, is small for a wide range of flow conditions of practical interest. We shall limit the discussion here to such cases. It is then clear that the weak radiative flux produced by the discontinuity in the temperature across the shock will cause the flow ahead of and behind the shock to change, such that profiles are obtained in all flow quantities. We shall calculate these profiles using a simple perturbation analysis of a hypersonic shock in a cool gas.

Taking the governing gasdynamic equations in the hypersonic approximation, and assuming for simplicity a perfect gas with constant specific heats, one can readily derive the following integral equation for the velocity across the shock

$$\frac{2\gamma}{\gamma - 1} u - \frac{\gamma + 1}{\gamma - 1} u^2 = 1 + \frac{4\sigma U_\infty{}^5}{\rho_\infty R^4} \int_{-\infty}^{+\infty} \times (u - u^2)^4 \operatorname{sgn}(\xi' - \xi) E_2(|\xi - \xi'|) d\xi' \quad (4)$$

where γ is the ratio of the specific heats, R the gas constant, U_∞ the unperturbed freestream velocity, ρ_∞ the unperturbed freestream density, and u is a nondimensional velocity equal to the actual velocity divided by U_∞. An equation similar in form to Eq. (4), but applicable in the entire supersonic range was derived and fully investigated by Heaslet and Baldwin.[2] If the radiative flux term is disregarded in Eq. (4), the velocity ahead of and behind the shock have the well-known values

$$\xi < 0: \ u = 1 \qquad \xi > 0: \ u = (\gamma - 1)/(\gamma + 1)$$

A weak radiative flux will perturb these values, such that we

Received January 21, 1965. This work was supported by the U. S. Air Force under Contract No. AF 04(695)-269.

* Member of the Technical Staff, Aerophysics Department, Aerodynamics and Propulsion Research Laboratory. Member AIAA.